ACS OMEGA

http://pubs.acs.org/journal/acsodf

Article

Comparative Saturation Binding Analysis of ^{64}Cu-Labeled Somatostatin Analogues Using Cell Homogenates and Intact Cells

Martin Ullrich,* Florian Brandt, Reik Löser, Jens Pietzsch, and Robert Wodtke*

Cite This: *ACS Omega* 2023, 8, 24003−24009

Read Online

ACCESS | Metrics & More | Article Recommendations | Supporting Information

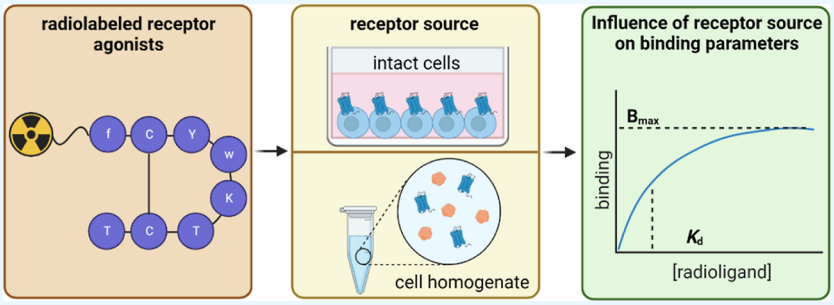

ABSTRACT: The development of novel ligands for G-protein-coupled receptors (GPCRs) typically entails the characterization of their binding affinity, which is often performed with radioligands in a competition or saturation binding assay format. Since GPCRs are transmembrane proteins, receptor samples for binding assays are prepared from tissue sections, cell membranes, cell homogenates, or intact cells. As part of our investigations on modulating the pharmacokinetics of radiolabeled peptides for improved theranostic targeting of neuroendocrine tumors with a high abundance of the somatostatin receptor sub-type 2 (SST_2), we characterized a series of ^{64}Cu-labeled [Tyr^3]octreotate (TATE) derivatives in vitro in saturation binding assays. Herein, we report on the SST_2 binding parameters measured toward intact mouse pheochromocytoma cells and corresponding cell homogenates and discuss the observed differences taking the physiology of SST_2 and GPCRs in general into account. Furthermore, we point out method-specific advantages and limitations.

INTRODUCTION

G-protein coupled receptors (GPCRs) are one of the most important pharmacological targets not only due to their involvement in a plethora of physiological processes but also due to an often well-defined and cell surface-exposed ligand binding site that enables the design of target molecules.[1,2] Moreover, GPCRs are attractive for the development of targeted radiopharmaceuticals for the diagnosis and therapy of tumors with radiolabeled agonists of the somatostatin receptor sub-type 2 (SST_2) as probably the most prominent examples.[3] In this context, [^{177}**Lu**]**Lu-DOTA-TATE** represents the first radiopharmaceutical for peptide receptor radionuclide therapy of neuroendocrine tumors, which has been approved by the EMA and FDA.[4] For the development of novel ligands targeting GPCRs including the elucidation of their pharmacological effects, initial characterization via binding and functional assays is necessary.[5] While the assessment of functional effects on cells upon ligand binding implies the use of intact cells (whole-cell assay format), binding studies, typically with the use of radioligands or fluorescent probes, are performed with different sources of the receptor, including tissue sections, membrane preparations, cell homogenates, and also intact cells.[6−12] In this context, there is a controversy about which of the receptor sources should be preferred with regard to the significance of the determined binding parameters, in particular when comparing cell homogenates and intact cells.[13−15]

Based on the vector molecule [Tyr^3]octreotate (TATE or TOCA) for SST_2 targeting, we recently reported on novel TATE derivatives modified with albumin binders ([^{64}**Cu**]**Cu-NODAGA-cLAB-TATEs**[16]), cleavage sequences for neprilysin, or both ([^{64}**Cu**]**Cu-NODAGA-NES-TATEs**[17]) to systematically explore the suitability of these structural modifications for modulating the pharmacokinetic properties of peptidic radioligands. As part of the in vitro radiopharmacological characterization, the SST_2 affinity of the [^{64}**Cu**]**Cu-NODAGA-cLAB-TATEs** was characterized in saturation binding analyses using cell homogenates of mouse pheochromocytoma cells (MPC) exhibiting high levels of SST_2.[18] For investigating the [^{64}**Cu**]**Cu-NODAGA-NES-TATEs**, we switched to intact cells instead of cell homogenates, primarily due to an occasionally high nonspecific binding when using cell homogenates. Having

Received: April 21, 2023
Accepted: June 9, 2023
Published: June 22, 2023

both methods established, we subsequently characterized a set of ten ^{64}Cu-labeled TATE derivatives comparing both MPC cell homogenates and intact cells. Herein, we report on the binding parameters obtained with the two different saturation binding assays and discuss the results considering the different assay formats when using cell homogenates and intact cells, the physiology of GPCRs, as well as the inherent limitations for determining the binding affinity of GPCR ligands.

RESULTS AND DISCUSSION

For a series of ten previously described ^{64}Cu-labeled TATE derivatives (Table 1), total and nonspecific binding to intact cells and cell homogenates were assessed over a range of radioligand concentrations. Exemplary saturation binding curves for one radioligand, **[^{64}Cu]Cu-NODAGA-NES5-TATE**, are shown in Figure 1A,B (for other radioligands, see Figure S1 in the Supporting Information). The calculated binding parameters K_d and B_{max} are summarized in Table 2. For the two assay formats employing cell homogenates and intact cells, radioligand binding was performed for 1 h at 37 °C. Generally, the K_d values toward both SST_2 sources were in a similar range but appeared to be systematically shifted to lower values when intact cells were used compared to cell homogenates. In contrast, the B_{max} values did not reveal such a trend. This is further exemplified by analyzing the K_d and B_{max} values with a ratio paired *t*-test (Figure 1C/D), which revealed that the logarithm of the K_d ratios is significantly different from 0 (i.e., the K_d ratios are different from 1, $p = 0.0005$) but not the B_{max} values ($p = 0.40$). The respective K_d ratios are listed in Table 2. The geometric mean of the K_d ratio is 2.41 (95% CI of 1.65−3.52). To rationalize the observed K_d shift, different aspects need to be considered that are discussed in the following sections.

Nonspecific Binding and Stability. As depicted in Figure 1A,B for **[^{64}Cu]Cu-NODAGA-NES5-TATE**, the extent of nonspecific binding to intact cells is reduced compared to the nonspecific binding to cell homogenates. This finding appears consistent among all compounds (Figure S1 in Supporting Information). In this context, it is worth noting that the data for total and nonspecific binding to the receptor sources were corrected for nonspecific binding to the well plates (in case of intact cells) and filter (in case of cell homogenates) as also outlined in the experimental descriptions. However, to validate that the extent of nonspecific binding is not caused by the different assay formats itself (washing in well plates versus filtration), the saturation binding assay was also performed for **[^{64}Cu]Cu-NODAGA-NES5-TATE** with intact cells in suspension under the conditions used for cell homogenates (Figure S2 in Supporting Information). The data indicate that the high nonspecific binding to cell homogenates is indeed caused by the receptor source itself as the nonspecific binding to intact cells under the same technical conditions is significantly lower. We hypothesize that this phenomenon originates from exposing the radioligand to cell components in cell homogenates that the radioligand does not encounter in intact cells due to its limited cell permeability.[14] This clearly favors the use of intact cells over cell homogenates as receptor source. However, the differences in nonspecific binding may not be responsible for the observed trend in the K_d values (e.g., due to potential limitations for data analysis) as radioligands such as **[^{64}Cu]Cu-DOTA-TATE** and **[^{64}Cu]Cu-NODAGA-TATE**, that show a low nonspecific binding for both receptor

Table 1. Summary of SST_2 Ligands Discussed Herein

compound	Chelator	N-terminal modification				SST_2 scaffold[a]
DOTA-TATE	DOTA					TATE
NODAGA-TATE	NODAGA-					TATE
NODAGA-Pra-PEG2-TATE	NODAGA-			Pra-	PEG2-	TATE
NODAGA-cLAB1-TATE	NODAGA- (X = N^{ε}-5-azidopentanoyl-N^{ε}-4-(4-iodophenyl)butanoyl-D-lysine)			Pra(X)[b]-	PEG2-	TATE
NODAGA-cLAB4-TATE	NODAGA- (X = N^{ε}-4-azidobenzoyl-N^{ε}-4-(4-methylphenyl)butanoyl-L-lysine amide)			Pra(X)[b]-	PEG2-	TATE
NODAGA-NES1-TATE	NODAGA-	Nle-	Val-	Lys(N3)-	PEG2-	TATE
NODAGA-NES2-TATE	NODAGA-	Nle-	Val-	Lys(N3)-	PEG2-	TATE
NODAGA-NES3-TATE	NODAGA-	Gly-	Phe-	Lys(N3)-	PEG2	TATE
NODAGA-NES4-TATE	NODAGA-	Gly-	Phe-	Lys(N3)-	PEG2	TATE
NODAGA-NES5-TATE	NODAGA- (X = N^{ε}-4-pentynoyl-N^{ε}-4-(4-iodophenyl)butanoyl-L-lysine)	D-Arg-	Gly-	Phe-	PEG2	TATE
NODAGA-JR11	NODAGA-	D-Arg-	Gly-	Lys(X)[b]-	PEG2	JR11

[a]TATE represents D-Phe-c(Cys-Tyr-D-Trp-Lys-Thr-Cys)-Thr-OH and JR11 represents Cpa-c(D-Cys-Aph(Hor)-D-Aph(Cbm)-Lys-Thr-Cys)-D-Tyr-NH_2. [b]The azide and alkyne functionalized albumin binders were coupled via on-resin CuAAC to the fully protected peptides bearing Pra and Lys(N_3) residues leading to a 1,4-disubstituted 1*H*-1,2,3-triazole linkage. For the synthesis and analytical data to NODAGA-JR11 see the Supporting Information. Aph, 4-aminophenylalanine; Cbm, carbamoyl; Cpa, 4-chlorophenylalanine; Hor, L-dihydroorotic acid; PAMBA, *p*-aminomethyl benzoic acid; Pra, L-propargylglycine.

https://doi.org/10.1021/acsomega.3c02755
ACS Omega 2023, 8, 24003−24009

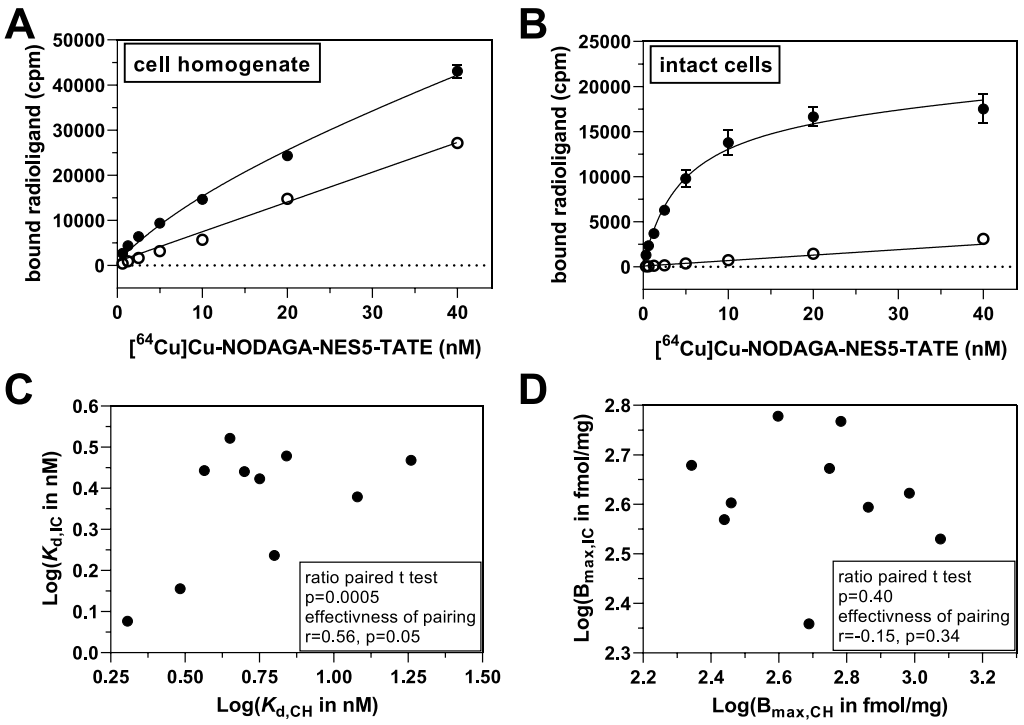

Figure 1. Comparison of saturation binding data using cell homogenates (CH) and intact cells (IC) (A/B) saturation binding of [^{64}Cu]Cu-NODAGA-NES5-TATE toward MPC cell homogenates (A) and intact cells (B) with data for total and nonspecific binding (in the presence of 1 μM DOTA-TATE) shown as filled and open circles, respectively. Plot in B was published recently by us (Adapted with permission from Brandt et al.[17] Copyright 2023, American Chemical Society). Regression analysis was performed by using the model of "one site—total and nonspecific binding" as implemented in GraphPad Prism (Version 9.4.1). (C,D) Correlation plots for the ratio paired t tests of K_d (C) and B_{max} (D) data with results of the tests given in the boxes.

Table 2. Summary of SST$_2$ Binding Data for a Series of ^{64}Cu-Labeled TATE Derivatives Using MPC Cell Homogenates and Intact MPC Cells

	MPC cell homogenate		intact MPC cells			
^{64}Cu-labeled compound[a]	K_d (nM)[b]	B_{max} (fmol/mg of protein)[b]	K_d (nM)[b]	B_{max} (fmol/mg of protein)[b]	uptake fraction (%)[c]	K_d ratio[e]
DOTA-TATE	2.03 (0.48)	562 (218)	1.19 (0.16)	471 (31)	56	1.70
TATE	3.05 (0.16)	965 (582)	1.43 (0.39)	420 (77)	64[d]	2.13
Pra-PEG2-TATE	4.48 (0.57)	488 (144)	3.33 (0.83)	229 (89)	48	1.35
cLAB1-TATE	6.31 (0.99)	1191 (334)	1.73 (0.35)	339 (73)	66	3.66
cLAB4-TATE	3.67 (3.30−4.09)[d]	396 (384−408)[d]	2.77 (0.62)	600 (50)	64	1.32
NES1-TATE	6.94 (6.19−7.78)	220 (212−229)	3.01 (0.65)	478 (175)	49[d]	2.31
NES2-TATE	18.2 (14.2−23.7)	288 (257−327)	2.94 (0.85)	401 (145)	56[d]	6.19
NES3-TATE	5.01 (4.04−6.20)	275 (257−294)	2.76 (2.33−3.25)[d]	371 (354−389)[d]	68[d]	1.82
NES4-TATE	5.64 (3.66−8.71)	606 (532−698)	2.65 (1.93−3.64)[d]	586 (532−649)[d]	53[d]	2.13
NES5-TATE	12.0 (1.50)	731 (189)	2.40 (1.34)	393 (190)	62[d]	5.01
JR11	5.35 (5.06−5.65)	764 (751−778)	8.17 (7.38−9.04)	717 (691−744)	28	0.65

[a]After ^{64}Cu-labeling, the non-labeled ligand was not separated or saturated with ^{nat}Cu^{2+}. [b]Data shown are mean values with calculated confidence interval of 68% of one experiment, which was performed in duplicate or triplicate, or mean values ±SEM of 2−3 or 6 (in case of [^{64}Cu]Cu-NODAGA-TATE toward intact MPC cells) experiments, which were also performed in duplicate or triplicate. [c]The uptake fraction ("internalized" or not acid releasable radioligand) is expressed as percentage of specific total-bound radioligand (Figure S4 in the Supporting Information). [d]Data were previously published by us (adapted with permission from Brandt et al.[16] Copyright 2022 American Chemical Society and Brandt et al.[17] Copyright 2023, American Chemical Society). [e]Ratio of K_d (cell homogenate)/K_d (intact cells). If not otherwise stated, the compounds bear NODAGA as chelator moiety for complexation of copper-64.

sources, also exhibit lower K_d values toward intact cells compared to cell homogenates.

Considering the aforementioned exposure of the radioligands to intracellular components in cell homogenates, a degradation by intracellular proteases could lead to reduced radioligand concentrations and thus apparently higher K_d values. While most of the serine and cysteine proteases might be inhibited by the used inhibitor cocktail during homogenization (see Materials and Methods), a residual proteolytic activity cannot be excluded. Therefore, for the two radioligands, [^{64}Cu]Cu-NODAGA-NES2-TATE and [^{64}Cu]Cu-NODAGA-NES5-TATE, the stability toward cell homogenates and intact cells under assay conditions were exemplarily examined (Figure S3 in the Supporting Informa-

https://doi.org/10.1021/acsomega.3c02755
ACS Omega 2023, 8, 24003−24009

tion). Both compounds remained comparably stable after 1 h of incubation to both receptor sources (≥87%) and thus, a proteolytic degradation might not contribute to the observed K_d shift.

Agonists versus Antagonists. The parent SST_2 ligand TATE is similar to octreotide or [Tyr^3]-octreotide, an agonist of the SST_2 receptor as previously characterized in functional assays assessing intracellular Ca^{2+}-release and uptake in intact cells for different TATE derivatives.[19−21] In line with these reports, the studied TATE derivatives herein showed a distinct uptake upon binding to SST_2 on MPC cells revealing uptake fractions between 48 and 68% after 1 h (Table 2). In order to investigate whether the observed difference in binding affinity is agonist-specific, we functionalized the known SST_2 antagonist **JR11**[22,23] with NODAGA and characterized its saturation binding and internalization behavior after ^{64}Cu-labeling using MPC cell homogenates and intact cells (Table 2). As expected for an antagonist, the uptake fraction was significantly lower (28%) compared to the TATE derivatives. Furthermore, the K_d value of **[^{64}Cu]Cu-NODAGA-JR11** was slightly lower in the cell homogenate assay compared to the intact cell assay (5.35 vs 8.17 nM), suggesting that the observed trend in the K_d values between the two sources of SST_2 might be specific for agonists.

Cellular Uptake and Sensitivity to Inorganic Ions. When using intact cells for radioligand binding, several aspects might complicate and affect the actual radioligand-receptor binding event.[24] These include the following: (1) receptor-mediated cellular uptake, (2) sensitivity to inorganic ions, and (3) activity status of the receptor.

Regarding cellular uptake, we already mentioned that this process occurs in MPC cells during the time span of the saturation binding experiments (Table 2). Potentially, receptor-mediated uptake lowers the apparent dissociation constant as the number of receptor-radioligand complexes at the cell surface are lowered causing a shift in the binding equilibrium at radioligand concentrations below receptor saturation to the side of the receptor−radioligand complex. Since uptake is considerably lower for antagonists, the binding affinity should be less affected by this process. In line with this consideration, the K_d value of the antagonist **[^{64}Cu]Cu-NODAGA-JR11** was similar in intact cells and cell homogenates.

Regarding the sensitivity to inorganic ions, Ribet and colleagues noted a pronounced Ca^{2+} sensitivity for the binding of ^{125}I-[Tyr^{11}]somatostatin to intact cells[25] and membranes[26] from guinea pig pancreatic acini. At low concentrations of Ca^{2+} (<100 nM), both K_d and B_{max} values increased 2−3-fold compared to those at optimal Ca^{2+} concentrations (>0.1 mM). In the present case, while the RPMI-1640 medium used for intact cells contains Ca^{2+} in a concentration of at least 0.4 mM,[27] the assay buffer used for the cell homogenates contains no added Ca^{2+}. Consequently, the different Ca^{2+} levels in binding assays with cell homogenates and intact cells could contribute to the observed trend in K_d values. Sodium ions are also known to regulate agonist binding to SST_2[28] with higher concentrations leading to a reduced binding affinity. However, the level of sodium ions in RPMI-1640 medium used for intact cells was much higher compared to the assay buffer used for cell homogenates, rendering the contribution of sodium ions to the K_d shift rather unlikely.

Activity Status of GPCRs. As for other proteins, GPCRs pass through a dynamic equilibrium of different conformational states, including their putatively active conformation (G-protein bound state), which is affected by various factors.[29] In terms of ligand binding, GPCRs attached to G-proteins generally exhibit a better affinity for agonists than the inactive state. A striking example for this can be found in a study of Florio and Sternweis, who observed a dramatic increase in binding potency of the agonist oxotremorine to muscarinic receptors in the presence of the G-protein G_0.[30] For adenosine A_{2A} and β_1-adrenoreceptors, it has been shown that the preference for the G-protein coupled receptor originates on a molecular basis from a narrower binding pocket and tighter contacts to the ligand upon G-protein binding.[31,32] For SST_2, recent structures obtained by cryo-electron microscopy for the inactive (apo-) receptor and the G-protein/octreotide-bound receptor suggest a similar phenomenon.[33,34] In line with this, the addition of GTP or GppNHp or pertussis toxin to membrane preparations of SST_2-synthesizing cells led to a marked reduction in the binding affinity of different radiolabeled agonists.[35−37] Consequently, as the GTP/GDP level might be lower in cell homogenates, the G-protein bound receptor state and thus agonist binding should actually be favored. In accordance with this consideration, Koenig et al.[38] characterized Neuro2A neuroblastoma cells regarding the binding of the selective SST_2 agonist [^{125}I]-BIM-23027 (c[N-Me-Ala-Tyr-D-Trp-Lys-Abu-Phe]) but were not able to determine both K_d and B_{max} values when using intact cells, which was related by the authors to high nonspecific binding but also the presence of a high GTP concentration in the cells. Moreover, Gerwins et al.[39] demonstrated in competition experiments that adenosine agonists bind to the adenosine A_1 receptor in membrane preparations according to a two-site model (low and high affinity site), while only a low affinity site could be detected upon binding to intact cells. The addition of GTP (100 μM) to the membrane preparations shifted the curve pattern to a one-site model and the obtained K_d values were in agreement with the K_d values obtained with intact cells. However, the results herein are in contrast to the aforementioned studies as the binding of the radioligands was even more favorable toward intact cells compared to cell homogenates. This could point to the fact that the SST_2 receptor in the MPC cells is in a large excess over the respective G-protein(s), rendering the fraction of G-protein-bound receptor less significant according to theoretical considerations.[40,41]

When discussing differences in ligand binding between different receptor sources, one should also consider the significance of the determined dissociation constants. There is the general view that measuring the binding affinity of GPCR agonists is always affected by the efficacy of the agonists,[40,42] which includes amongst others receptor-mediated uptake and G-protein binding. This brings us to the point that the applied assay conditions for neither the cell homogenates nor the intact cells might provide experimentally determined dissociation constants (also named K_{obs}) according to the classic definition of the dissociation constants (K_d) since G-protein binding among others was not prevented from the outset. However, considering that, e.g., receptor-mediated uptake of radiolabeled SST_2 agonists also occurs in vivo,[43,44] intact cells might represent, from our perspective, a better physiological model for the evaluation of the radioligand performance. We would also like to point out in this context, that after ^{64}Cu-labeling of the TATE derivatives, separation of the non-labeled ligand was not performed. Consequently, the data shown in

https://doi.org/10.1021/acsomega.3c02755
ACS Omega 2023, 8, 24003−24009

Table 2 are obtained for a mixture of ^{64}Cu-labeled and non-labeled ligands with apparent molar activity[45] values in the range of 20−50 GBq/μmol. We are aware that this certainly led to an altered binding affinity compared to the pure metal complexes as previously shown by Reubi et al.[46] However, the separation of radioligands is typically not required for preclinical and clinical applications (provided the molar activity is sufficiently high). Therefore, we have omitted radioligand separation for the in vitro binding experiments.

CONCLUSIONS

Overall, the use of intact MPC cells instead of cell homogenates provides an appropriate assay for assessing the binding properties of newly developed ligands to SST_2. The tendency in binding affinities appears conserved between cell homogenates and intact cell, but the nonspecific binding to intact cells is markedly reduced compared to the nonspecific binding to cell homogenates. The general trend to lower binding affinities toward intact cells cannot be fully rationalized but appears to be agonist-specific and might arise from several aspects, with the concurrent cellular uptake and the potential Ca^{2+} sensitivity of SST_2 being just two potential explanations. The pharmacological effects of agonist binding toward SST_2 on MPC cells will be further explored complemented by comparisons to human cells with a high abundance of SST_2.

MATERIALS AND METHODS

Radiolabeling of DOTA/NODAGA-Bearing Peptides.[16,17] [^{64}Cu]$CuCl_2$ was produced at the Helmholtz-Zentrum Dresden-Rossendorf on the 30 MeV TR-Flex-Cylotron (Advanced Cyclotron Systems Inc., ACSI, Canada) by a ^{64}Ni(p,n)^{64}Cu nuclear reaction as reported previously.[47,48]

For a typical radiolabeling procedure, 550 MBq of [^{64}Cu]$CuCl_2$ (60 μL in H_2O) was mixed with 0.01 M HCl (230 μL) and ammonium acetate buffer (2 M, pH 8, 30 μL) to obtain a solution with a pH value around 5.5. An aliquot of this mixture (105 μL) was then added to the peptide stock solution (2.5 μL of 2 mM in 10% DMSO/PBS, pH 7.4), and the mixture was incubated for 20 min at 60−80 °C. Quality control of the radiolabeled peptide conjugates was performed by radio-HPLC analysis.[16,17] Labeling yields were usually ≥97%. The radiolabeled peptides were used without purification. Molar activities of up to 50 GBq/μmol were achieved and were calculated based on the applied peptide amount. For further binding experiments, the reaction mixture was diluted with cell culture medium or phosphate buffered saline (PBS, pH 7.4).

In Vitro SST_2 Binding Affinity Using MPC Cell Homogenates.[16] MPC cells (passages 35−40) were routinely cultured in collagen-coated flasks as described elsewhere[49] and harvested at 70−80% confluency in Dulbecco's phosphate-buffered saline containing 2.0 mM ethylenediaminetetraacetic acid (EDTA) at 4 °C for 30 min. Cells were resuspended and frozen in fetal bovine serum containing 10% (v/v) DMSO and stored at −70 °C. After thawing, cells were washed and resuspended in ice-cold saturation assays buffer, pH 7.4, containing 50 mM Tris-HCl, 1 mM EDTA, 0.5 mM *o*-phenanthroline, and 0.1% (w/v) bovine serum albumin. Cells were homogenized in ice-cold saturation assay buffer supplemented with complete EDTA-free proteinase inhibitor (Roche, Basel Switzerland) using a Dounce homogenizer. Protein content of cell homogenates was measured at A_{280nm} (setting 1 Abs = 1 mg/mL) using a nanodrop spectrophotometer (Thermo-Fisher Scientific).

For the measurement of total binding, 0.155 mL of cell homogenates were incubated with radioligands (molar activity (A_m) = 25 MBq/nmol) at increasing final concentrations between 0.625 and 40 nM (final sample volume 0.2 mL) in Polystyrene tubes (5 mL, round bottom, clear, Greiner bio-one, Item no. 115101). For the measurement of nonspecific binding, specific binding sites were saturated with non-labeled DOTA-TATE at a final concentration of 1 μM. Samples were incubated for 60 min at 37 °C. Incubation was stopped by soaking cell homogenates into Whatman GF/C collection filters (GE Healthcare, Chicago, IL, USA; presoaked in 0.3% (v/v) polyethyleneimine for 90 min) and washing with ice-cold Dulbecco's phosphate-buffered saline using a cell harvester (Brandel, Gaithersburg, MD, USA). Nonspecific binding of the radioligands (at 0.312, 1.25, 5, and 20 nM, with and without 1 μM of non-labeled DOTA-TATE; the values at the other radioligand concentrations were derived by linear regression) to the filters was assessed in the absence of cell homogenates. Activity bound to filters was measured using the gamma counter Wizard (PerkinElmer). Activity in a series of radioligand standards was measured at increasing molar amounts between 0.625 and 40 nM. Measurements for total binding were performed in duplicate, while single measurements were performed for nonspecific binding.

In Vitro SST_2 Binding Affinity Using Intact MPC Cells.[17] A number of 3 × 10^5 cells/cm^2 were seeded in collagen-coated 48-well microplates (CELLSTAR 48 Well Cell Culture Multiwell Plates, Polystyrene, Greiner bio-one, Item no. 677180) and grown for three days. For binding assays, cell culture medium was removed and replaced by fresh medium supplemented with the radioligand (A_m = 25 MBq/nmol) at increasing final concentrations between 0.321 and 40 nM (final sample volume 0.2 mL). Nonspecific cell binding was measured in the presence of non-labeled DOTA-TATE at a final concentration of 1 μM. Nonspecific binding to plastic surfaces was determined in cell-free wells at radioligand concentrations of 0.312, 1.25, 5, and 20 nM (with and without 1 μM non-labeled DOTA-TATE; the values at the other radioligand concentrations were derived by linear regression). Samples were incubated for 60 min at 37 °C. Incubation was stopped by washing with ice-cold Dulbecco's PBS. Cells were lysed with 0.1 M NaOH containing 1% (w/v) SDS. Activity was measured in cell homogenates and in a series of radioligand standards containing increasing molar amounts between 0.06 and 8 pmol using the gamma counter Wizard (PerkinElmer). Protein content of cell homogenates was measured as described above. Measurements for total binding were performed in triplicate, while measurements for non-specific binding were performed in duplicates.

Determination of K_d and B_{max} Values. Plots of "total binding" = f(radioligand) were analyzed by nonlinear regressions using the model of "one site—total, accounting for ligand depletion" as implemented in GraphPad Prism and Plots of "nonspecific binding" = f(radioligand) were analyzed by linear regressions. For the ligand depletion model, the term "NS" was constrained to the respective slopes obtained by the linear regressions. The terms "SpecAct" (obtained with standard curves) and "Vol" (0.2 mL, assay volume for both SST_2 sources) were also constrained. K_d values were derived in nM, and the B_{max} values (in cpm) were transformed into fmol/mg. Both data sets were corrected for nonspecific binding, i.e.,

https://doi.org/10.1021/acsomega.3c02755
ACS Omega 2023, 8, 24003−24009

binding to the Whatman GF/C collection filters (in the absence of cell homogenate) or binding to the microplate cavities (in the absence of intact cells).

Cell Binding and Uptake. MPC cells were seeded into collagen-coated 24-well microplates and cultivated for 4 days. All washing steps were performed using PBS containing 0.9 mM $CaCl_2$ and 0.5 mM $MgCl_2$. Total radioligand uptake was measured after incubation with the radioligand (A_m = 30 GBq/μmol) at a final concentration of 20 nM in RPMI 1640 medium with GlutaMAX supplement (Thermo Fisher Scientific) for 1 h at 37 and 4 °C. Nonspecific binding was determined in the presence of 20 μM Acetyl-TATE. The uptake fraction was measured after acid wash of cell surface-bound radioligand with wash buffer containing 0.05 M glycine, pH 2.8, for 5 min. The activity of cell homogenates was measured using the γ counter Wizard (PerkinElmer). The protein content of cell homogenates was measured as described above.

■ ASSOCIATED CONTENT

Supporting Information

The Supporting Information is available free of charge at https://pubs.acs.org/doi/10.1021/acsomega.3c02755.

Synthesis and characterization of NODAGA-JR11 and [^{64}Cu]Cu-NODAGA-JR11 saturation binding curves for the ^{64}Cu-labeled TATE derivatives and [^{64}Cu]Cu-NODAGA-JR11; comparison of assay settings for [^{64}Cu]Cu-NODAGA-NES5-TATE; stability toward cell homogenate and intact cells; and cell binding data for the ^{64}Cu-labeled TATE derivatives (PDF)

■ AUTHOR INFORMATION

Corresponding Authors

Martin Ullrich − *Helmholtz-Zentrum Dresden-Rossendorf, Institute of Radiopharmaceutical Cancer Research, Dresden 01328, Germany*; Email: m.ullrich@hzdr.de

Robert Wodtke − *Helmholtz-Zentrum Dresden-Rossendorf, Institute of Radiopharmaceutical Cancer Research, Dresden 01328, Germany*; orcid.org/0000-0001-7462-7111; Email: r.wodtke@hzdr.de

Authors

Florian Brandt − *Helmholtz-Zentrum Dresden-Rossendorf, Institute of Radiopharmaceutical Cancer Research, Dresden 01328, Germany; School of Science, Faculty of Chemistry and Food Chemistry, Technische Universität Dresden, Dresden 01069, Germany*

Reik Löser − *Helmholtz-Zentrum Dresden-Rossendorf, Institute of Radiopharmaceutical Cancer Research, Dresden 01328, Germany; School of Science, Faculty of Chemistry and Food Chemistry, Technische Universität Dresden, Dresden 01069, Germany*; orcid.org/0000-0003-1531-7601

Jens Pietzsch − *Helmholtz-Zentrum Dresden-Rossendorf, Institute of Radiopharmaceutical Cancer Research, Dresden 01328, Germany; School of Science, Faculty of Chemistry and Food Chemistry, Technische Universität Dresden, Dresden 01069, Germany*; orcid.org/0000-0002-1610-1493

Complete contact information is available at: https://pubs.acs.org/10.1021/acsomega.3c02755

Notes

The authors declare no competing financial interest.

The TOC graphic was created with biorender.com.

■ ACKNOWLEDGMENTS

This research was funded by Deutsche Forschungsgemeinschaft (DFG) within the Collaborative Research Center Transregio 205/1 and 205/2 "The Adrenal: Central Relay in Health and Disease" (CRC/TRR 205/1 and 205/2; M.U. and J.P.). We cordially appreciate the expert support of Andrea Suhr for performing ^{64}Cu-labeling and the various radiometric assay methods. We thank Dr. Martin Kreller and the cyclotron team as well as Dr. Martin Walther and Christian Jentschel for providing [^{64}Cu]$CuCl_2$. The excellent technical assistance of Mareike Barth regarding cell culture is greatly acknowledged. MPC 4/30PRR cells were kindly provided by Arthur Tischler, James Powers, and Karel Pacak.

■ REFERENCES

(1) Hauser, A. S.; Attwood, M. M.; Rask-Andersen, M.; Schioth, H. B.; Gloriam, D. E. Trends in GPCR drug discovery: new agents, targets and indications. *Nat. Rev. Drug Discovery* **2017**, *16*, 829−842.

(2) Jacoby, E.; Bouhelal, R.; Gerspacher, M.; Seuwen, K. The 7 TM G-protein-coupled receptor target family. *ChemMedChem* **2006**, *1*, 760−782.

(3) Franco Machado, J.; Silva, R. D.; Melo, R.; Correia, J. Less exploited GPCRs in precision medicine: targets for molecular imaging and theranostics. *Molecules* **2018**, *24*, 49.

(4) Hennrich, U.; Kopka, K. Lutathera®: The First FDA- and EMA-Approved Radiopharmaceutical for Peptide Receptor Radionuclide Therapy. *Pharmaceuticals* **2019**, *12*, 114.

(5) Kenakin, T. P. Cellular assays as portals to seven-transmembrane receptor-based drug discovery. *Nat. Rev. Drug Discovery* **2009**, *8*, 617−626.

(6) McKinney, M.; Raddatz, R. Practical aspects of radioligand binding. *Curr. Protoc. Pharmacol.* **2006**, *33*, 1.3.1.

(7) Bylund, D. B.; Toews, M. L. Radioligand binding methods for membrane preparations and intact cells. *Receptor signal transduction protocols. Methods in Molecular Biology*; Willars, G., Challiss, R., Eds.; Humana Press: Totowa, NJ, 2011; Vol. *746*, pp 135−164.

(8) Maguire, J. J.; Kuc, R. E.; Davenport, A. P. Radioligand binding assays and their analysis. In *Receptor binding techniques*; Davenport, A., Ed.; Methods in Molecular Biology; Humana Press: Totowa, NJ, 2012; Vol. *897*, pp 31−77. https://www.ncbi.nlm.nih.gov/pubmed/22674160.

(9) Flanagan, C. A. GPCR-radioligand binding assays. *Methods Cell Biol.* **2016**, *132*, 191−215.

(10) Müller, C.; Gleixner, J.; Tahk, M. J.; Kopanchuk, S.; Laasfeld, T.; Weinhart, M.; Schollmeyer, D.; Betschart, M. U.; Lüdeke, S.; Koch, P.; Rinken, A.; Keller, M. Structure-Based Design of High-Affinity Fluorescent Probes for the Neuropeptide Y Y(1) Receptor. *J. Med. Chem.* **2022**, *65*, 4832−4853.

(11) Soave, M.; Briddon, S. J.; Hill, S. J.; Stoddart, L. A. Fluorescent ligands: Bringing light to emerging GPCR paradigms. *Br. J. Pharmacol.* **2020**, *177*, 978−991.

(12) Stoddart, L. A.; White, C. W.; Nguyen, K.; Hill, S. J.; Pfleger, K. D. Fluorescence- and bioluminescence-based approaches to study GPCR ligand binding. *Br. J. Pharmacol.* **2016**, *173*, 3028−3037.

(13) Motulsky, H. J.; Mahan, L. C.; Ansel, P. A. Radioligand, agonists and membrane-receptors on intact cells - data analysis in a bind. *Trends Pharmacol. Sci.* **1985**, *6*, 317−319.

(14) Vauquelin, G.; Van Liefde, I.; Swinney, D. C. Radioligand binding to intact cells as a tool for extended drug screening in a representative physiological context. *Drug Discov. Today Technol.* **2015**, *17*, 28−34.

(15) Sykes, D. A.; Stoddart, L. A.; Kilpatrick, L. E.; Hill, S. J. Binding kinetics of ligands acting at GPCRs. *Mol. Cell. Endocrinol.* **2019**, *485*, 9−19.

(16) Brandt, F.; Ullrich, M.; Laube, M.; Kopka, K.; Bachmann, M.; Löser, R.; Pietzsch, J.; Pietzsch, H. J.; van den Hoff, J.; Wodtke, R. Clickable albumin binders for modulating the tumor uptake of targeted radiopharmaceuticals. *J. Med. Chem.* **2022**, *65*, 710−733.
(17) Brandt, F.; Ullrich, M.; Wodtke, J.; Kopka, K.; Bachmann, M.; Löser, R.; Pietzsch, J.; Pietzsch, H. J.; Wodtke, R. Enzymological Characterization of ^{64}Cu-Labeled Neprilysin Substrates and Their Application for Modulating the Renal Clearance of Targeted Radiopharmaceuticals. *J. Med. Chem.* **2023**, *66*, 516−537.
(18) Ullrich, M.; Bergmann, R.; Peitzsch, M.; Zenker, E. F.; Cartellieri, M.; Bachmann, M.; Ehrhart-Bornstein, M.; Block, N. L.; Schally, A. V.; Eisenhofer, G.; Bornstein, S. R.; Pietzsch, J.; Ziegler, C. G. Multimodal somatostatin receptor theranostics using [^{64}Cu]Cu-/[^{177}Lu]Lu-DOTA-(Tyr^3)octreotate and AN-238 in a mouse pheochromocytoma model. *Theranostics* **2016**, *6*, 650−665.
(19) Schottelius, M.; Reubi, J. C.; Eltschinger, V.; Schwaiger, M.; Wester, H. J. N-terminal sugar conjugation and C-terminal Thr-for-Thr(ol) exchange in radioiodinated Tyr3-octreotide: effect on cellular ligand trafficking in vitro and tumor accumulation in vivo. *J. Med. Chem.* **2005**, *48*, 2778−2789.
(20) Leyton, J.; Iddon, L.; Perumal, M.; Indrevoll, B.; Glaser, M.; Robins, E.; George, A. J.; Cuthbertson, A.; Luthra, S. K.; Aboagye, E. O. Targeting somatostatin receptors: preclinical evaluation of novel 18F-fluoroethyltriazole-Tyr3-octreotate analogs for PET. *J. Nucl. Med.* **2011**, *52*, 1441−1448.
(21) Mansi, R.; Plas, P.; Vauquelin, G.; Fani, M. Distinct In Vitro Binding Profile of the Somatostatin Receptor Subtype 2 Antagonist [^{177}Lu]Lu-OPS201 Compared to the Agonist [^{177}Lu]Lu-DOTA-TATE. *Pharmaceuticals* **2021**, *14*, 1265.
(22) Cescato, R.; Erchegyi, J.; Waser, B.; Piccand, V.; Maecke, H. R.; Rivier, J. E.; Reubi, J. C. Design and in vitro characterization of highly sst2-selective somatostatin antagonists suitable for radiotargeting. *J. Med. Chem.* **2008**, *51*, 4030−4037.
(23) Rylova, S. N.; Stoykow, C.; Del Pozzo, L.; Abiraj, K.; Tamma, M. L.; Kiefer, Y.; Fani, M.; Maecke, H. R. The somatostatin receptor 2 antagonist ^{64}Cu-NODAGA-JR11 outperforms ^{64}Cu-DOTA-TATE in a mouse xenograft model. *PLoS One* **2018**, *13*, No. e0195802.
(24) Koening, J. A. Radioligand Binding in Intact cells. In *Methods in Molecular Biology - Receptor Binding Techniques*; Keen, M., Ed.; Humana Press: Totowa, New Jersey, 1999; pp 89−98.
(25) Taparel, D.; Esteve, J. P.; Susini, C.; Vaysse, N.; Balas, D.; Berthon, G.; Wunsch, E.; Ribet, A. Binding of somatostatin to guinea-pig pancreatic membranes: regulation by ions. *Biochem. Biophys. Res. Commun.* **1983**, *115*, 827−833.
(26) Esteve, J. P.; Susini, C.; Vaysse, N.; Antoniotti, H.; Wunsch, E.; Berthon, G.; Ribet, A. Binding of somatostatin to pancreatic acinar cells. *Am. J. Physiol.* **1984**, *247*, G62−G69.
(27) https://www.thermofisher.com/de/de/home/technical-resources/media-formulation.114.html (accessed March 07, 2023).
(28) Kong, H.; Raynor, K.; Yasuda, K.; Bell, G. I.; Reisine, T. Mutation of an aspartate at residue 89 in somatostatin receptor subtype 2 prevents Na+ regulation of agonist binding but does not alter receptor-G protein association. *Mol. Pharm.* **1993**, *44*, 380−384.
(29) Weis, W. I.; Kobilka, B. K. The molecular basis of G protein-coupled receptor activation. *Annu. Rev. Biochem.* **2018**, *87*, 897−919.
(30) Florio, V. A.; Sternweis, P. C. Mechanisms of muscarinic receptor action on G_o in reconstituted phospholipid vesicles. *J. Biol. Chem.* **1989**, *264*, 3909−3915.
(31) Lee, S.; Nivedha, A. K.; Tate, C. G.; Vaidehi, N. Dynamic role of the G protein in stabilizing the active state of the adenosine A_{2A} receptor. *Structure* **2019**, *27*, 703−712.e3.
(32) Warne, T.; Edwards, P. C.; Dore, A. S.; Leslie, A. G. W.; Tate, C. G. Molecular basis for high-affinity agonist binding in GPCRs. *Science* **2019**, *364*, 775−778.
(33) Robertson, M. J.; Papasergi-Scott, M. M.; He, F.; Seven, A. B.; Meyerowitz, J. G.; Panova, O.; Peroto, M. C.; Che, T.; Skiniotis, G. Structure determination of inactive-state GPCRs with a universal nanobody. *Nat. Struct. Mol. Biol.* **2022**, *29*, 1188−1195.
(34) Robertson, M. J.; Meyerowitz, J. G.; Panova, O.; Borrelli, K.; Skiniotis, G. Plasticity in ligand recognition at somatostatin receptors. *Nat. Struct. Mol. Biol.* **2022**, *29*, 210−217.
(35) Hershberger, R. E.; Newman, B. L.; Florio, T.; Bunzow, J.; Civelli, O.; Li, X. J.; Forte, M.; Stork, P. J. The somatostatin receptors SSTR1 and SSTR2 are coupled to inhibition of adenylyl cyclase in Chinese hamster ovary cells via pertussis toxin-sensitive pathways. *Endocrinology* **1994**, *134*, 1277−1285.
(36) Koenig, J. A.; Edwardson, J. M.; Humphrey, P. P. Somatostatin receptors in Neuro2A neuroblastoma cells: operational characteristics. *Br. J. Pharmacol.* **1997**, *120*, 45−51.
(37) Siehler, S.; Seuwen, K.; Hoyer, D. Characterisation of human recombinant somatostatin receptors. 1. Radioligand binding studies. *Naunyn-Schmiedebergs Arch. Pharmakol.* **1999**, *360*, 488−499.
(38) Koenig, J. A.; Edwardson, J. M.; Humphrey, P. P. Somatostatin receptors in Neuro2A neuroblastoma cells: ligand internalization. *Br. J. Pharmacol.* **1997**, *120*, 52−59.
(39) Gerwins, P.; Nordstedt, C.; Fredholm, B. B. Characterization of adenosine A1 receptors in intact DDT1 MF-2 smooth muscle cells. *Mol. Pharmacol.* **1990**, *38*, 660−666.
(40) Strange, P. G. Agonist binding, agonist affinity and agonist efficacy at G protein-coupled receptors. *Br. J. Pharmacol.* **2008**, *153*, 1353−1363.
(41) Kenakin, T. P. *Pharmacologic Analysis of Drug-Receptor Interactions*, 3rd ed.; Lippincott-Raven Publishers: Philadelphia, 1997; pp 242−288.
(42) Colquhoun, D. Binding, gating, affinity and efficacy: the interpretation of structure-activity relationships for agonists and of the effects of mutating receptors. *Br. J. Pharmacol.* **1998**, *125*, 923−947.
(43) Waser, B.; Tamma, M. L.; Cescato, R.; Maecke, H. R.; Reubi, J. C. Highly efficient in vivo agonist-induced internalization of sst2 receptors in somatostatin target tissues. *J. Nucl. Med.* **2009**, *50*, 936−941.
(44) Reubi, J. C.; Waser, B.; Cescato, R.; Gloor, B.; Stettler, C.; Christ, E. Internalized somatostatin receptor subtype 2 in neuroendocrine tumors of octreotide-treated patients. *J. Clin. Endocrinol. Metab.* **2010**, *95*, 2343−2350.
(45) Luurtsema, G.; Pichler, V.; Bongarzone, S.; Seimbille, Y.; Elsinga, P.; Gee, A.; Vercouillie, J. EANM guideline for harmonisation on molar activity or specific activity of radiopharmaceuticals: impact on safety and imaging quality. *EJNMMI Radiopharm. Chem.* **2021**, *6*, 34.
(46) Reubi, J. C.; Schär, J. C.; Waser, B.; Wenger, S.; Heppeler, A.; Schmitt, J. S.; Mäcke, H. R. Affinity profiles for human somatostatin receptor subtypes SST1-SST5 of somatostatin radiotracers selected for scintigraphic and radiotherapeutic use. *Eur. J. Nucl. Med.* **2000**, *27*, 273−282.
(47) Kreller, M.; Pietzsch, H.; Walther, M.; Tietze, H.; Kaever, P.; Knieß, T.; Füchtner, F.; Steinbach, J.; Preusche, S. Introduction of the new center for radiopharmaceutical cancer research at Helmholtz-Zentrum Dresden-Rossendorf. *Instruments* **2019**, *3*, 9.
(48) Thieme, S.; Walther, M.; Pietzsch, H. J.; Henniger, J.; Preusche, S.; Mäding, P.; Steinbach, J. Module-assisted preparation of ^{64}Cu with high specific activity. *Appl. Radiat. Isot.* **2012**, *70*, 602−608.
(49) Ullrich, M.; Bergmann, R.; Peitzsch, M.; Cartellieri, M.; Qin, N.; Ehrhart-Bornstein, M.; Block, N. L.; Schally, A. V.; Pietzsch, J.; Eisenhofer, G.; Bornstein, S. R.; Ziegler, C. G. In vivo fluorescence imaging and urinary monoamines as surrogate biomarkers of disease progression in a mouse model of pheochromocytoma. *Endocrinology* **2014**, *155*, 4149−4156.

https://doi.org/10.1021/acsomega.3c02755
ACS Omega 2023, 8, 24003−24009